

1 **A review of the potential for rare earth element resources from European red**
2 **muds: examples from Seydişehir, Turkey and Parnassus-Giona, Greece**

3 Éimear A. Deady^{1*}, Evangelos Mouchos², Kathryn Goodenough³, Ben J.
4 Williamson² and Frances Wall²

5 ¹British Geological Survey, Environmental Science Centre, Nicker Hill, Keyworth,
6 Nottingham, NG12 5GG, UK

7 ²Camborne School of Mines, College of Engineering, Mathematics and Physical
8 Sciences, University of Exeter, Penryn Campus, Penryn, Cornwall, TR10 9FE, UK

9 ³British Geological Survey, Murchison House, West Mains Road, Edinburgh, EH9
10 3LA, UK

11 Corresponding authors email address: eimear@bgs.ac.uk

12 **Abstract**

13 Rare earth elements (REE) are viewed as ‘critical metals’ due to a complex array of
14 production and political issues, most notably a near monopoly in supply from China.
15 Red mud, the waste product of the Bayer process that produces alumina from
16 bauxite, represents a potential secondary resource of REE. Karst-bauxite deposits
17 represent the ideal source material for REE-enriched red mud as the conditions
18 during formation of the bauxite allow for the retention of REE. The REE pass
19 through the Bayer Process and are concentrated in the waste material. Millions of
20 tonnes of red mud are currently stockpiled in onshore storage facilities across
21 Europe, representing a potential REE resource. Red mud from two case study sites,

22 one in Greece and the other in Turkey, has been found to contain an average of
23 approximately 1000 ppm total REE, with an enrichment of light over heavy REE.
24 Although this is relatively low grade when compared with typical primary REE
25 deposits (Mountain Pass and Mount Weld up to 80000ppm), it is of interest because
26 of the large volumes available, the cost benefits of reprocessing waste, and the low
27 proportion of contained radioactive elements. This work shows that around 12000
28 tonnes of REE exist in red mud at the two case study areas alone, with much larger
29 resources existing across Europe as a whole.

30 **Introduction**

31 Processing of the primary aluminium ore, bauxite, to produce alumina (Al_2O_3) using
32 the Bayer process produces a waste material known as red mud. Long term storage
33 of this is expensive and represents an environmental risk, as demonstrated by
34 disasters such as the red mud dam failure at Kolontár, Hungary which caused
35 extensive damage to neighbouring land and waterways and the death of nine
36 people (Gelencsér *et al.*, 2011; Milačič *et al.*, 2012; Anton *et al.*, 2014). To mitigate
37 this risk, as well as to reduce cost, a number of studies have been undertaken to
38 identify possible uses for red mud (e.g. Klauber *et al.*, 2011; Power *et al.*, 2011;
39 Binnemans *et al.*, 2013a).

40

41 Annual global extraction of bauxite in 2013 (the last year for which figures are
42 available) was approximately 296 million tonnes (Mt), up 16% from 2012 (BGS,
43 2015). Annually, this results in the production of approximately 150 Mt of red mud

44 (IAI, 2014). Decades of work on the valorisation of red muds have not yet found a
45 significant alternative use for this voluminous waste product (Klauber *et al.*, 2011).
46 Only around 2 Mt (~1.6% of the global total) is currently used each year (Ritter,
47 2014), mostly in construction materials, as cement additives and in brick making
48 (Klauber *et al.*, 2011).

49

50 The Bayer process produces virtually pure alumina (> 99% Al₂O₃) and therefore
51 almost all non-alumina ‘impurities’ from the original bauxite end up in the red mud
52 waste. These ‘impurities’ have been found to include significant amounts of
53 gallium, scandium and REE (Ochsenkühn-Petropoulou *et al.*, 1995, 1996; Smirnov
54 and Molchanova, 1997; Akcil *et al.*, 2013; Rusal, 2014; Borra *et al.*, 2015). Ga and
55 the REE are classed as ‘critical metals’ (EC, 2014) i.e. those having limited global
56 distribution of production, no known substitutes, highly specialised applications
57 and being of economic significance (Graedel *et al.*, 2014).

58 REE are generally divided into light REE (LREE) from lanthanum to samarium and
59 heavy REE (HREE) from europium to lutetium; Yttrium behaves as a HREE due to its
60 similar physical and chemical properties (Wall, 2014). HREE, followed by LREE, are
61 classified by the European Commission (EC, 2014) and British Geological Survey
62 (BGS, 2012) as the most ‘critical’ of all raw materials. They are deemed essential to
63 the economies of Canada, Japan and the US among others (CREEN, 2013;
64 Humphries, 2013; Mitsubishi Electric, 2014). Annual global production of REE
65 (expressed as rare earth oxides (REO)), was approximately 100170 t in 2013 (BGS,

66 2015). Of this, over 90% was supplied by China. This geospatial concentration of
67 production has raised concerns over security of supply (Hatch, 2012).

68 The REE are now essential to many green and modern technologies such as smart-
69 phone screens, electric cars and wind turbines (Wall, 2014). This has led to
70 increasing global demand for REE with demand growth of 5.6% between 1970 and
71 2010 (Alonso *et al.*, 2012). Present development of electric vehicles and wind
72 turbines relies heavily on dysprosium and neodymium for rare-earth magnets.
73 Future adoption of these technologies may result in large and disproportionate
74 increases in the demand for these two elements (Alonso *et al.*, 2012). Economic
75 exploitation of REE from primary deposits, such as alkaline magmatic rocks,
76 carbonatites and ion adsorption clays, is dependent on the ratio of LREE to HREE in
77 the deposit and metallurgical characteristics of the REE present (Simandl, 2014).
78 Alternative sources of REE are becoming more important due to a range of factors
79 including increasing demand, a poorly developed REE recycling industry (Simandl,
80 2014), a more volatile supply chain from China (Hatch, 2012), and the 'balance
81 problem', where demand for specific elements and the natural abundance of those
82 elements in deposits are 'unbalanced', resulting in excess supply of less in-demand
83 REE (Binnemans *et al.*, 2013b; Binnemans and Jones, 2015). In the European Union
84 (EU) this has led to the seventh framework programme (FP7) funding of the EURARE
85 (European Rare Earth Resources, www.eurare.eu) project which aims to research
86 and develop European resources and production of REE in a sustainable,
87 economically viable and environmentally friendly way. Europe in this context refers

88 to the EU-28, Liechtenstein, Iceland, Norway and Switzerland, and the candidate
89 and potential candidate countries. Russia and Ukraine are not included in this work.

90 Primary resources of REE have been identified and explored across Europe over the
91 past decades (Goodenough *et al.*, 2016), such as at Norra Kärr, Sweden; Fen,
92 Norway; the Kvanefjeld and Kringlerne deposits in Greenland; and the Aksu Dıamas
93 deposit in Turkey. However, none have so far gone into production. Attention has
94 also turned to secondary sources, mainly from the recycling or processing of waste
95 materials. Europe's red muds represent one such possible resource. The work
96 presented here aims to assess the REE potential of European red muds. The study
97 is based on two case examples, Seydişehir, Turkey and Parnassus-Giona, Greece,
98 where the parent karst-bauxites have been identified as REE-bearing (Ochsenkühn-
99 Petropoulou *et al.*, 1991; Laskou and Andreou, 2003; Karadağ *et al.*, 2009), and the
100 red muds are stored in accessible 'dry' piles or tailing ponds. These case studies are
101 put in the context of a review of European red mud resources where resource
102 estimates of available REE in European red mud storage facilities are presented.

103 **Bauxites and alumina in Europe**

104 Within Europe, bauxite is currently extracted in six countries: Bosnia and
105 Herzegovina, France, Greece, Hungary, Montenegro and Turkey. Production in
106 2013 equalled almost 3.5 Mt, approximately 1% of global production (BGS, 2015).
107 Historically, bauxite has been exploited more widely across Europe, particularly in
108 the Mediterranean region (Figure 1), representing a significant proportion of global
109 bauxite production (~15% in 1974 (IGS, 1978)). There are three main categories of

110 bauxite deposit (Bárdossy, 1982): 1. Lateritic bauxite deposits, which derive from *in*
111 *situ* weathering of aluminosilicate rocks; 2. Karst bauxite deposits, which occur in
112 the karst topography of limestone and dolomite and comprise aluminosilicate
113 residues that have been transported from either proximal or distal locations; 3.
114 Tikhvin-type deposits, which are laid down on aluminosilicate rocks but have no
115 genetic relationship to them. Karst bauxite deposits can be subdivided further into
116 six main types (Bárdossy, 1982; Bosák *et al.*, 1989), of which the 'Mediterranean
117 type' karst bauxite deposits are of the most interest in Europe due to the amount
118 of REE present. Red mud waste from these Mediterranean bauxite types is the
119 focus of this paper.

120 Formation of karst bauxites begins with muddy sediments being washed into
121 hollows in karst topography. These sediments are subsequently bauxitised through
122 deep lateritic weathering. Bauxitisation is facilitated by moderate temperatures
123 and through-put of mildly alkaline fluids, which allow silica to be incongruently
124 dissolved from minerals such as feldspar and kaolinite leaving an aluminium-rich
125 residue (Gow and Lozej, 1993; Bland and Rolls, 1998). Alongside this, Al may
126 accumulate from a variety of sources including the insoluble residue of limestone,
127 other aluminosilicate material (volcanic ash and clay layers) within the limestone,
128 or the erosion, transportation and weathering of aluminosilicate rocks. The main
129 Al-bearing minerals in bauxite are the monohydrates boehmite ($\gamma\text{-AlO}(\text{OH})$) and
130 diaspore ($\alpha\text{-AlO}(\text{OH})$), and the trihydrate gibbsite ($\text{Al}(\text{OH})_3$). The main gangue
131 minerals include hematite (Fe_2O_3), goethite ($\text{FeO}(\text{OH})$), anatase (TiO_2), kaolinite
132 ($\text{Al}_2\text{Si}_2\text{O}_5(\text{OH})_4$) and minor quartz (SiO_2).

133 The process of bauxitisation progresses from the top downwards and laterally
134 outward following the direction of drainage (Bárdossy, 1982). Karst-bauxite
135 typically forms under moderate temperatures in subtropical climates usually with
136 an average mean temperature of 26°C (Bárdossy, 1979). Good drainage of slightly
137 alkaline fluids through the developing bauxite is essential for formation. It has been
138 shown that the major element chemical composition of bauxites varies from one
139 region to another and within individual deposits (Akinic and Artir, 2008). The
140 formation conditions also have an important influence on the REE content and
141 distribution within the bauxite. The sources and formation conditions of selected
142 European karst-bauxite deposits, and the implications that these may have for REE
143 content, are discussed below. The size and grade of bauxite deposits is dependent
144 on the duration of the weathering (Bogatyrev *et al.*, 2009), but the effect of the
145 duration of weathering on the REE content is unclear.

146 Alumina production from bauxite has been on-going in Europe since the
147 development of the Bayer process over 125 years ago. To separate alumina from
148 bauxite, the ore is digested in a hot sodium hydroxide solution to convert the
149 alumina to aluminium hydroxide, which dissolves in the hydroxide liquor. The other
150 components of bauxite do not dissolve. The solution is clarified by filtering off the
151 solid impurities, which forms the bauxite residue or red mud (Hind *et al.*, 1999). The
152 composition of red muds depends on the nature of the parent bauxite, the mining
153 location and the parameters of the Bayer process (Hind *et al.*, 1999).
154 Mineralogically, red mud is mainly composed of red coloured iron oxides in the
155 form of hematite (Fe_2O_3) and maghemite ($\gamma\text{-Fe}_2\text{O}_3$), aluminium oxides in the form

156 of diaspore ($\alpha\text{-AlO}(\text{OH})$) and gibbsite ($\text{Al}(\text{OH})_3$), and silicon, calcium, sodium and
157 titanium oxides such as calcite (CaCO_3), silicon calcium aluminate hydroxide
158 ($\text{Ca}_3\text{Al}_2(\text{SiO}_4)(\text{OH})_8$), perovskite (CaTiO_3), rutile (TiO_2) and cancrinite
159 ($\text{Na}_6\text{Ca}_2\text{Al}_6\text{Si}_6\text{O}_{24}(\text{CO}_3)_2 \cdot 2\text{H}_2\text{O}$) (Atasoy, 2007). Red muds typically have a density of
160 around 2.75 g/cm^3 and a pH of > 12 .

161 Red muds are produced at a rate of approximately 150 Mt per year globally. There
162 are now approximately 60 alumina refineries worldwide outside China using the
163 Bayer process, of which 10 are located in Europe (Figure 2). An additional 49
164 refineries were operating in China in 2011 (IAI, 2014). European refineries produce
165 alumina from both European and imported bauxite in order to supply the needs of
166 the European market. The importation of bauxite from a wide range of sources
167 makes it difficult to assess the REE content of the resulting red mud waste. In
168 Europe, the largest alumina refinery is Aughinish in the Republic of Ireland, which
169 has an output of 1.93 Mt of alumina per annum. Each tonne of alumina produced
170 results in the formation of between 0.7 and 2 tonnes of red mud (IAI, 2014).
171 Assuming an average overall ratio of 1:1.5 alumina to red mud (Hamada, 1986;
172 Power *et al.*, 2011), the Aughinish plant is likely to produce almost 3 Mt of red mud
173 per annum.

174 Worldwide, an estimated 2.7 billion tonnes (Bt) of red muds have been produced
175 since the development of the Bayer process (Power *et al.*, 2011). These have been
176 treated in a variety of ways, including storage in onshore lagoons and direct marine
177 disposal (Power *et al.*, 2011). Historically, large quantities of the waste material

178 were directly dumped into the sea, however, this practice has been regulated under
179 the 'Convention on the Prevention of Marine Pollution by Dumping of Wastes and
180 Other Matter (IMO, 1972)', the 'London Convention' for short. The practice of
181 disposal at sea is expected to be completely abandoned by 2016 (IAI, 2014). Most
182 commonly, red muds are stored in settling ponds onshore in closed cycle disposal
183 systems; no alumina refineries built after 1970 are known to employ marine
184 disposal of red muds (Power *et al.*, 2011).

185 Statistics on European alumina production since 1972 have been gathered from the
186 British Geological Survey's World mineral statistics database and are shown in
187 Figure 3. Greek production before 2009 is not included, as before then red muds
188 were disposed of at sea. The quantities of red muds likely to have been produced
189 annually in Europe and stored onshore since the introduction of the 'London
190 Convention' have been estimated as at least 200 000 t, using a minimum ratio of
191 1:0.7 tonnes of alumina to residue and a maximum ratio of 1:2 tonnes of alumina
192 to residue, with an average ratio of 1:1.5 tonnes of alumina used (Figure 3).

193 **Rare earth elements in bauxite**

194 The characterisation of REE-containing minerals in bauxites was pioneered in the
195 1970s (Bárdossy and Pantó, 1973; Maksimović and Roaldset, 1976; Maksimović and
196 Pantó, 1978; Vukotić, 1983). Of historical note was the first identification of
197 secondary minerals of the bastnäsite group in the San Giovanni Rotondo bauxite in
198 Italy (Bárdossy and Pantó, 1973). Since then, both authigenic and detrital REE-
199 bearing minerals have been found in bauxites. The most common authigenic REE-

200 bearing mineral is hydroxylbastnäsite-(Nd) ($\text{Nd}(\text{CO}_3)(\text{OH})$), while monazite
201 ($(\text{Ce},\text{La},\text{Nd},\text{Th})\text{PO}_4$) is the most common detrital REE-bearing mineral (Maksimović
202 and Pantó, 1996). In some occurrences the presence of detrital minerals can result
203 in high REE values, e.g. at Nagyharsány, a Hungarian monazite-bearing bauxite
204 which has total REE (*TREE*) of up to 10000 ppm (Bárdossy *et al.*, 1976). The leaching
205 of monazite in this deposit led to the precipitation of authigenic bastnäsite-group
206 minerals near the base of the bauxite (Bárdossy *et al.*, 1976; Maksimović and Pantó,
207 1996). In an example from the Southern Apennines of Italy, detrital monazite,
208 xenotime (YPO_4), and supergene LREE-enriched phosphates (high Ce, low La-Nd,
209 Ca minerals and florencite-type $(\text{REE})\text{Al}_3(\text{PO}_4)_2(\text{OH})_6$ minerals) derived from the
210 weathering of monazite were detected in bauxite using SEM-EDS and QEMSCAN®
211 (Mondillo *et al.*, 2011; Boni *et al.*, 2013). In addition, bauxites from the Southern
212 Apennines (Italy) (Boni *et al.*, 2013) and Nurra (Sardinia) (Mameli *et al.*, 2007)
213 contain authigenic high-Ce, Ca-bearing fluorcarbonate minerals $(\text{REE}_2\text{Ca}(\text{CO}_3)_3\text{F}_2)$.
214 Parisite $(\text{Ca}(\text{Ce},\text{La})_2(\text{CO}_3)_3\text{F}_2)$ has previously been identified in the basal parts of the
215 Spinazzola bauxite in Italy (Mongelli, 1997; Mongelli and Acquafredda, 1999),
216 however, recent analysis suggests that parisite occurs homogeneously throughout
217 the deposit (Mongelli *et al.*, 2014).

218 Fractionation of LREE and HREE has been noted in many Mediterranean bauxites
219 (Maksimović and Pantó, 1991; Mongelli, 1997; Laskou and Economou-Eliopoulos,
220 2007; Karadağ *et al.*, 2009; Boni *et al.*, 2013), resulting in vertical separation of REE
221 in bauxite profiles (Boni *et al.*, 2013). Fractionation of Ce, which behaves differently
222 to the other REE, in particular in the uppermost parts of bauxite, is as a result of the

223 supergene oxidation of Ce^{+3} to Ce^{+4} . This allows precipitation of cerianite
224 ($(Ce^{4+},Th)O_2$) to occur, with resultant Ce-depleted fluids percolating through the
225 system. Scavenging by iron oxide phases, such as goethite (Boni *et al.*, 2013), of Ce-
226 depleted fluids results in further fractionation of REE between the ooids (concentric
227 particles of bauxite with a diameter of between 100 and 1000 μm (Bárdossy, 1982))
228 and matrix of the bauxite in basal parts of the bauxite (Mongelli, 1997). Subsequent
229 dissolution of cerianite under acidic conditions and *per descensum* transport of REE
230 can result in the precipitation of LREE-rich minerals, such as parisite, at the base of
231 the deposit (Mongelli, 1997; Mameli *et al.*, 2007). Parisite in particular precipitates
232 under alkaline conditions, such as those found at the base of the bauxite due to the
233 alkaline aquifers in the underlying limestone. Parisite precipitation throughout a
234 bauxite deposits, such as in the Spinazzola bauxite, can be explained by cyclical
235 changes in water table levels and subsequent changes in Eh and pH (Mongelli *et al.*,
236 2014).

237 Preferential uptake of REE by both iron and manganese mineral phases has been
238 identified in other systems such as in marine ferromanganese deposits (Ohta and
239 Kawabe, 2001) and in river estuary systems where iron oxyhydroxide adsorption of
240 LREE in particular occurs (Marmolejo-Rodríguez *et al.*, 2007). The alkaline 'pH
241 barrier' created by the underlying limestone aquifer influences the stability of the
242 REE-carbonate complexes that form at the base of the deposit (Johannesson *et al.*,
243 1995, 1996). As the stability of these complexes increases with atomic number, the
244 HREE are preferentially retained in solution as carbonate complexes. The
245 distribution of the REE along this 'pH barrier' is heterogeneous and they can be

246 concentrated in lenses and micropores, space fillings and microveins (Maksimović
247 and Pantó, 1996).

248 **Rare earth elements in red muds**

249 REE are concentrated into red muds through the Bayer process (Wagh and Pinnock,
250 1987) which results from the association of REE with iron and titanium phases
251 which pass through unchanged (Derevyankin *et al.*, 1981). To illustrate this, red
252 muds from lateritic-type Timan bauxites in Russia have been shown to contain up
253 to 90% of the Nb, Sc and REE present in the original bauxite (Klyucharev *et al.*,
254 2013). Similarly, Ochsenkühn-Petropoulou *et al.* (1994) and Wagh and Pinnock
255 (1987) have demonstrated up to two-fold increases in REE, including Sc and Y, in
256 red muds when compared to the bulk chemistry of the Greek and Jamaican source
257 bauxites, respectively.

258 The minerals known to occur in red muds include some that are produced during
259 the Bayer process, e.g. desilicification products such as sodalite ($\text{Na}_8(\text{Al}_6\text{Si}_6\text{O}_{24})\text{Cl}_2$),
260 cancrinite ($\text{Na}_6\text{Ca}_2\text{Al}_6\text{Si}_6\text{O}_{24}(\text{CO}_3)_2 \cdot 2\text{H}_2\text{O}$) and Na-aluminosilicate, and calcite (Atasoy,
261 2007). However, most minerals are unaltered residual phases from the original
262 bauxite such as monazite, bastnäsite, hematite (Fe_2O_3), diaspore ($(\alpha\text{-AlO}(\text{OH}))$),
263 gibbsite ($\text{Al}(\text{OH})_3$) and quartz (SiO_2) (Power *et al.*, 2011).

264 The mineralogy and petrology of REE-bearing minerals in red muds are relatively
265 poorly constrained (Ochsenkühn-Petropoulou *et al.*, 1996; Borra *et al.*, 2015).
266 Scavenging of REE by iron oxyhydroxides is observed in bauxites (Mongelli, 1997;

267 Mongelli and Acquafredda, 1999; Boni *et al.*, 2013), however, the distribution of
268 REE phases in red muds is less well understood. An association between REE and
269 Sc with iron oxides in red muds has been observed through leaching studies (Borra
270 *et al.*, 2015 and references therein). Sc is heterogeneously distributed through the
271 red muds, being mainly contained within detrital mineral phases, such as the Sc-
272 enriched zircons found in bauxite (Boni *et al.*, 2013). It may also either be adsorbed
273 onto the surface of iron oxide phases or enriched in the outer layers of iron oxide
274 particles (Borra *et al.*, 2015), which may be the same in the case of REE.

275 The Bayer process involves many steps that affect the characteristics of the red
276 muds and hence potentially the REE distribution within the residue. Milling of the
277 bauxite ore initially changes the particle size and surface area of the minerals, which
278 has an impact on the settling rates within the red mud lagoons, and can also affect
279 chemical properties such as adsorption and dissolution of minerals. It is not possible
280 to apply a general enrichment factor for REE to red muds; it is necessary to
281 investigate the REE enrichment in each red mud locality and compare this, where
282 possible, with the parent bauxite. Further work to define the distribution of REE
283 within red muds is necessary in order to develop a clearer understanding of both
284 the distribution of REE and the phases that host REE within red muds.

285 Recent advances in the valorisation of red muds for minor metals include the
286 development of Rusal's pilot plant in the Urals, Russia, which is capable of
287 producing 2.5 t/a primary scandium oxide concentrate (RUSAL, 2014). Binnemans
288 *et al.* (2013a) give an overview of current methods of REE extraction from red muds.

289 Bench scale extraction of REE from dehydrated red muds using imidazolium-based
290 ionic liquids is being researched through the EURARE project at National Technical
291 University of Athens (NTUA) (Bourbos *et al.*, 2014; Davris *et al.*, 2014) while
292 leaching experiments are on-going at KU Leuven, Belgium (Borra *et al.*, 2015). The
293 commercial extraction of REE from red muds has been further advanced by the
294 granting of a patent in both Canada and the US to Orbite Aluminae for the ‘Orbite
295 Process’, (Patent No. 14/371,364, Orbite, 2015), which uses red muds as a
296 feedstock for a new beneficiation stream that aims to extract REE and other minor
297 metals along with alumina, magnesium oxide and titanium dioxide from the
298 residue. It is thus clear that red muds have the potential to be a source for REE for
299 the European economy.

300 **European red muds, case studies**

301 The Mediterranean region has a complex geological history shaped most recently
302 by the closure of the Lower Palaeozoic to Cenozoic Palaeotethys and Neotethys
303 oceanic system which existed between the continents of Eurasia and Gondwana
304 (Robertson and Mountrakis, 2006). Continental collision resulted in the formation
305 of the Dinarides-Hellenides-Taurides orogenic belt, which extends across the
306 Eastern Mediterranean region, and which includes many carbonate units that
307 provide the karst topography in which karst bauxites have formed. The regional
308 geology is summarised below briefly to set the geological context for the bauxite
309 precursors of the case study localities.

310 **Sampling and analytical methodology**

311 Four samples of red muds (14/T/15-19) were collected at a depth of approximately
312 20 cm from different locations within the waste ponds at the ETİ Alüminyum S.A.
313 processing plant in Seydişehir, Turkey (inset Figure 4). The samples comprised 300
314 g of wet red muds; each individual sample consisted of three subsamples, which
315 were later recombined and dried. Preparation and analysis of the samples was
316 carried out at the British Geological Survey, Keyworth, Nottingham. Samples were
317 fused with sodium peroxide and 0.2 g of the resulting glass digested with dilute HCl
318 acid and then, HF acid. Dilute sample solutions (in 1% HNO₃+ 0.5% HCL) were then
319 analysed for 56 trace elements in an Agilent 7500CX series ICP-MS. Data for a
320 duplicate analysis of sample 14/T/16, for all elements, were within 0.18%. Data for
321 international standards (AGV-2 (andesite produced by USGS), BCR-2 (Columbia
322 River Basalt produced by USGS) and JR-2 (produced by Geological Survey of Japan))
323 were always within 6% of published values.

324 Samples of Greek red muds were collected from dewatered stockpiles at the
325 Aluminium S.A. alumina refinery in Agios Nikolaos. Three samples, equating to
326 approximately 5 kg in total, were taken at three different locations (13/Gr/A,
327 13/Gr/B and 13/Gr/Z) across the area of the stockpiled residue. Each of the samples
328 represent red mud residue from different deposits, mined at different times.
329 Preparation of the samples was carried out at the Camborne School of Mines,
330 Penryn, Cornwall. Five grams of each sample were analysed for 31 trace elements
331 (LF100 analysis) by ICP-MS, following lithium borate fusions at Bureau Veritas
332 Minerals Laboratories (BVML), Canada. International standards, BX-N bauxite
333 (reference material produced by ANRT (Association Nationale de la Recherche

334 Technique)) and STD SO-18 were used by BVML. Values obtained were within 2.7%
335 of published values. Data from blank samples were checked for contamination and
336 detection limits. Duplicate analyses (n = 1) of, sample 13/Gr/B were within $\pm 0.5\%$.
337 Results are presented in Table 1, see supplemental data for duplicate, corrections
338 and certified reference material data.

339 **Case studies: red muds from Seydişehir, Turkey and Parnassus-Giona, Greece**

340 *Case study one: red muds from Seydişehir, Turkey*

341 *Geology*

342 The Anatolide-Tauride terrane is one of three main terranes into which
343 Turkey is subdivided (Şengör and Yılmaz, 1981). The terrane shows Gondwana
344 affinities but was separated from the main mass of Gondwana by the southern
345 branch of Neo-Tethys in the Triassic. Upper Triassic to Upper Cretaceous carbonate
346 deposition formed several thousand metres of thick shallow marine carbonate
347 deposits on a passive margin (Okay, 2008), which have subsequently been
348 overthrust by Upper Cretaceous limestone and ophiolitic material. The karst
349 topography formed on the carbonates in this region hosts a large number of
350 bauxite, Al-laterite and manganese deposits which are mainly Upper Cretaceous to
351 Cenozoic in age. The Mortaş and Doğankuzu Mediterranean-type karst bauxites are
352 located in the central Tauride Mountains, close to Seydişehir, and are hosted in
353 fossiliferous limestones of the Upper Cretaceous Mortaş Formation (Figure 4)
354 (Temur *et al.*, 2009).

355 Both the Doğankuzu and Mortaş bauxites are mined to provide feedstock for the
356 alumina refinery at Seydişehir. The Mortaş deposit is lens shaped, 950 m in length
357 and 350 m wide, and the adjacent Doğankuzu bauxite elongate, with a strike length
358 of approximately 900 m and a width of 50 m (Karadağ *et al.*, 2009). The deposits
359 occur between 1500 and 2000 m above sea level. The bauxites can be subdivided
360 into four horizons: massive bauxite, oolitic bauxite, breccia-bearing bauxite and
361 earthy bauxite. The main Al-bearing mineral is boehmite, with minor diasporite and
362 anatase, while the main accessory minerals are hematite, kaolinite and goethite.
363 REE are most enriched in the massive and oolitic bauxite horizons relative to the
364 hosting limestone (Karadağ *et al.*, 2009). Bauxite deposition is thought to have
365 resulted from mass flow triggered by tectonic activity with transport of weathered
366 'bauxitic soil' over short distances into depressions and sinkholes in the limestone
367 (Öztürk *et al.*, 2002). The bauxite deposits are between 1 and 40 m thick, and are
368 overlain by thin layers of claystone and argillaceous limestone. These are in turn
369 overlain by c. 50 m of Santonian massive limestone, with an overlying thick cover
370 of bioclastic limestone of Upper Cretaceous age and Eocene limestone and flysch.
371 The bauxites therefore must have formed in a depositional hiatus during the Upper
372 Cretaceous (Öztürk *et al.*, 2002).

373 *Bauxite deposits and red muds*

374 The Seydişehir bauxite deposits of Mortaş and Doğankuzu have a total
375 resource of 26.3 Mt high-alumina boehmite bauxite at 55–67% Al₂O₃, of which
376 approximately 6 Mt had been mined by 2002 (Öztürk *et al.*, 2002; Horkel, 2010).

377 These, the two largest bauxite open pits in Turkey, supply the only aluminium
378 smelter in the country (Horkel, 2010), currently operated by ETİ Alüminyum.
379 Bauxite is mined from April to October annually and stockpiled at their plant in
380 Seydişehir; extraction during the winter is suspended due to the inclement weather
381 in the mountains. The extracted bauxite from the two mines is blended to create a
382 plant feed with aluminium content suitable for processing at Seydişehir. Annual
383 production is approximately 800 000 t of bauxite (BGS, 2015), generating
384 approximately 1.5 Mt of red mud. Approximately 10 Mt are stockpiled in the tailing
385 ponds. The red muds collected in the tailing ponds are waste material from both
386 bauxite pits. It is not therefore possible to determine the relative contribution of
387 REE from each of the deposits to the red mud samples.

388 *Case study two: red muds from Parnassus-Giona, Greece*

389 *Geology*

390 Greece is geologically subdivided into several tectonic zones, representing
391 an amalgamation of terranes accreted over an extended period from the Lower
392 Palaeozoic to the Mesozoic. The External Hellenides resulted from the Early
393 Tertiary destruction of a Neotethyan oceanic strand known as the Pindos Ocean,
394 which led to the collision between the Apulian and Pelagonian microcontinents
395 (Doutsos *et al.*, 2006 and references therein). The Parnassus-Giona zone is located
396 within the External Hellenides, which is limited to Central Greece and consists
397 almost entirely of limestone and dolomite of Mesozoic age (Doutsos *et al.*, 2006).

398 The Parnassus-Giona tectonic zone is characterised by a nearly continuous
399 sequence of Upper Triassic to Upper Cretaceous epicontinental reef-like
400 carbonates. At the time of formation the Parnassus-Giona zone was a shallow
401 lagoon, with both freshwater and seawater ingress due to changing tectonic and
402 climatic conditions (Valeton *et al.*, 1987). Several phases of uplift, with associated
403 marine transgressions and regressions, permitted the creation of multiple bauxite
404 horizons during the Jurassic and Cretaceous. The materials which formed the
405 bauxites in this area are thought to have been transported by sedimentary
406 processes over a calcareous terrain for a distance of over 30 km (Petrascheck,
407 1989). The bauxite horizons, termed B1-B3, from oldest to youngest, formed during
408 the Upper Jurassic to Middle Cretaceous (Figure 5) (Valeton *et al.*, 1987, Laskou *et*
409 *al.*, 2010). These bauxite deposits comprise lenses, pockets and irregular masses.
410 The economically most important deposits occur in the B3 horizon which is laterally
411 extensive as a continuous layer with a thickness of between one and ten metres
412 (Petrascheck and Mack, 1978; Valeton *et al.*, 1987; Melfos and Voudouris, 2012;
413 Tsirambides and Filippidis, 2012; Laskou and Economou-Eliopoulos, 2013). REE-
414 bearing minerals occur in very small concentrations within the bauxites (Valeton *et*
415 *al.*, 1987). The mineral grains are small (between 1 and 10 μm) and can be
416 authigenic, detrital, or material from weathered parent lithologies (Bárdossy *et al.*,
417 1976). LREE-bearing minerals include phosphates, such as detrital rhabdophane-
418 (Ce) $((\text{Ce},\text{La})\text{PO}_4(\text{H}_2\text{O}))$ and florencite-(Ce) $(\text{CeAl}_3(\text{PO}_4)_2(\text{OH})_6)$, whereas HREE-
419 bearing minerals are Y-phosphates such as detrital churchite $(\text{YPO}_4 \cdot 2\text{H}_2\text{O})$ and
420 xenotime (Laskou and Andreou, 2003). Monazite and secondary bastnäsité-group

421 minerals, such as hydroxylbastnäsite-(Nd) and hydroxylbastnäsite-(La)
422 ((La)CO₃(OH,F)), and parisite-group minerals occur as micropore and fissure filling
423 aggregates (Lymeropoulou, 1996; Maksimović and Pantó, 1996; Gamaletsos *et al.*,
424 2007).

425 Coal layers, with a maximum thickness of 50 cm, are found in some locations just
426 above the B3 horizon, covered by limestone of Upper Cretaceous age forming the
427 thick layers of the Parnassus-Giona Unit (Kalaitzidis *et al.*, 2010). Oxidation of pyrite
428 inclusions in the coal resulted in the formation of acid fluids that percolated
429 downwards to cause bleaching of the upper parts of the underlying bauxite
430 (Kalaitzidis *et al.*, 2010). This may have impacted on the distribution of REE within
431 the bauxite, as under acidic conditions REE are easily weathered from
432 aluminosilicates (Nesbitt, 1979; Fleet, 1984; Karadağ *et al.*, 2009).

433 *Bauxite production and red muds*

434 The karst bauxite deposits of Greece are among the world's most important
435 sources of bauxite for non-metallurgical products such as for chemicals and fused
436 alumina. The main exploitable deposits are those in the Parnassus-Giona zone, with
437 indicated reserves of 100 Mt (O'Driscoll, 2011). Bauxite production is
438 predominantly from underground mining of the B3 horizon, with less from the
439 deeper B2 horizons. The B1 horizon is currently not being exploited due to its
440 greater depth. Alumina is refined at the Aluminium S.A. site using the Bayer process
441 and the resulting waste red muds (700000 tpa (Anagnostou, 2010)) are dewatered

442 and stockpiled onshore. Deposition of dewatered red mud started in 2009; the
443 approximate total volume accumulated to end 2015 is 5 Mt.

444 **Bauxite REE geochemistry**

445 Previous work on the Mortaş bauxite from Turkey (Karadağ *et al.*, 2009; Haniççi,
446 2013) and the Parnassus-Giona bauxites from Greece (Ochsenkühn-Petropoulou *et*
447 *al.*, 1991, 1994, 1995; Lyemperopoulou, 1996; Valeton *et al.*, 1987; Laskou, 1991,
448 2005; Laskou *et al.*, 2010; Laskou and Economou-Eliopoulos, 2007, 2013), shows
449 that they are enriched in the LREE relative to the HREE (Figure 6; Table 1). The
450 Mortaş bauxites show a clear negative europium (Eu) anomaly on a chondrite-
451 normalised plot (Figure 6), whilst the Greek bauxites only display a small negative
452 Eu anomaly. These anomalies are likely to be inherited from the bauxite protoliths.
453 The Greek bauxites show a positive Ce anomaly that is not present in the Mortaş
454 bauxite. The Ce anomaly could be due to samples being collected from higher, near
455 surface, relatively oxidising conditions where Ce is dominantly present as Ce⁴⁺,
456 rather than Ce³⁺, and therefore fixed in oxides. Laskou and Andreou (2003) also
457 identified a positive Ce anomaly in samples from the upper (B3) and middle (B2)
458 bauxite horizons. Overall the Mortaş bauxite is more enriched in the REE (614 ppm
459 *TREE* (Karadağ *et al.*, 2009)) than the Greek bauxite (B3 horizon averages from 417
460 ppm (Valeton *et al.*, 1987; [Economopolou-Kyriakopoulou, 1991]; Laskou, 1991,
461 2005; Ochsenkühn-Petropoulou *et al.*, 1991; Laskou and Economou-Eliopoulos,
462 2007, 2013) to 527 ppm *TREE* (mixed bauxite from the B3 and B2 horizons sampled
463 at the processing plant) (Ochsenkühn-Petropulu *et al.*, 1994, 1995)); again this

464 could be due to sampling bias as the Greek samples were collected mostly from
465 higher horizons. Published data for karst-bauxite deposits from Italy (Boni *et al.*,
466 2013) and Turkey (Karadağ *et al.*, 2009; Haniççi, 2013) show similar trends in REE
467 content (Table 1), displaying relative enrichments in the LREE, particularly for Nd
468 and Ce.

469

470 **Results: rare earth element content of red muds**

471 All the sampled red muds show moderate enrichment in *TREE* (by up to 1.9 times,
472 Figure 6) when compared with the original bauxite (Figure 6; Table 1), with the
473 exception of 14/T/15. Small negative Eu anomalies in all red mud samples are likely
474 to have been inherited from the bauxite protolith. Small positive Gd anomalies are
475 also present in the red muds from both Greece and Turkey, but only occur in one
476 bauxite sample (Greece B3 horizon). The values for REE in the parent bauxites are
477 taken from the literature and will not necessarily correspond exactly to the specific
478 red mud sample being analysed.

479 Turkish red mud samples 14/T/16, 14/T/18 and 14/T/19 have an average content
480 of 1 090 ppm *TREE*, and are all relatively enriched in REE compared with the
481 published values for the parent bauxites (Figure 6; Table 1). Sample 14/T/15,
482 however, shows an overall depletion in REE relative to the Mortaş bauxite (*TREE*
483 150 ppm). This may be because this sample was taken from the far west end of the
484 pond (inset Figure 4), where the red mud cover is thin and therefore meteoric
485 waters may have leached out the REE, or alternatively, the sample may have come

486 from an unusually low REE bauxite feedstock. Turkish red mud samples 14/T/15-16
487 and 14/T/19 show a positive Ce anomaly, whilst sample 14/T/18 shows a negative
488 Ce anomaly. This could be due to the oxidation state of Ce in the bauxite horizon
489 from which the waste was derived. Sample 14/T/18 also has higher total HREE
490 content, 356 ppm compared with an average of 208 ppm, which could also be
491 explained if it was sourced from deeper within the bauxite. Within the bauxite
492 profile, HREE complexes are more stable in the more alkaline conditions that occur
493 at depth during bauxite formation (Johannesson *et al.*, 1995, 1996; Mameli *et al.*,
494 2007).

495 Greek red mud samples show similar REE patterns to the Turkish samples though
496 they are generally less enriched in REE (Table 1; Figure 6). They also show a more
497 homogeneous spatial distribution of REE, even though samples are from different
498 mines within the B3 and occasionally the B2 layers. *TREE* values range between 800-
499 900 ppm (up to 1000 ppm where Sc is included). All samples are characterised by
500 Ce, La, Nd and Y enrichments. Distinct positive Ce and negative Eu anomalies are
501 visible with minor enrichments in Tb and Gd also present. It should be noted that
502 the samples have been individually analysed by slightly different methods and in
503 different laboratories and as such are not directly comparable. However, these are
504 representative samples from two large red mud storage facilities and so can be
505 used to give an insight into European REE resources from alternative sources.

506

507 **Resource potential**

508 Whether red mud in Europe represents a potential resource for REE will largely
509 depend on whether proven bench- and pilot-scale processing and beneficiation
510 techniques for this material can be up-scaled for production. For a detailed
511 overview of these, readers are directed to Binnemans *et al.*, 2015. In addition, a
512 clear understanding of the volume of red muds present in Europe will aid in
513 assessing whether these resources are viable. The remaining discussion will focus
514 on this second aspect.

515 Table 2 utilises the data from Figure 3 and Table 1 to estimate *TREE* to calculate
516 average total contained REE, Nd and HREE in the red muds of Europe. Taking an
517 average value of 1000 ppm REE in red mud gives a range of resource potentials in
518 Europe. If the REE were to be extracted at an efficiency of 50% (Ochsenkühn-
519 Petropoulou *et al.*, 1996), then the minimum quantity of available REE would be 100
520 000 t, while at a maximum there are approximately 270 000 t REE in European red
521 muds. 425 Mt of red mud (see average cumulative figure in Table 2) at 1000 ppm
522 REE would contain 430 000 t of REE, which at 50% recovery could produce 210 000 t
523 REE. These figures are based on stored red mud stocks produced from alumina
524 refining in Europe since 1972, and as such, are a conservative estimate for the
525 potential resources available from red muds in Europe.

526 In a global context, around 150 Mt of red muds are currently being produced per
527 year with up to 150 000 t of contained REE going to waste ponds. This equates to
528 approximately 172 500 t REO, using 1.15 as an average element-to-stoichiometric
529 oxide conversion factor. Annual global production of REE, expressed as tonnes of
530 REO, was approximately 100 170 t in 2013 (BGS, 2015). It is thus clear that there is
531 potential for red muds to make a substantial contribution to the global supply of
532 REE.

533 Taking neodymium as an example, the potential Nd resources in red muds across
534 Europe is approximately 20000 - 45000 t. This equates to greater than four years of
535 global production, calculated at approximately 23000 t per year (2011 data) (EC,
536 2013 and references therein). The figures from Europe as a whole indicate that
537 HREE (Eu to Lu +Y) resources in red muds could be as much as 60000 t. With the
538 development of selective beneficiation techniques it may be possible to prevent
539 the oversupply of LREE as is the current market situation (in 2015), and
540 preferentially produce the more in-demand elements such as neodymium and
541 dysprosium. An important caveat is that these figures represent red mud waste
542 from all bauxite types processed in European refineries. Annual importation of
543 bauxite into Europe equalled more than 13.5 Mt in 2013, (the last year for which
544 figures are available) (BGS, 2015), with major import partners including Guinea and
545 Brazil (data from UN Comtrade Database, accessed May 2015). Major bauxite
546 deposits in these countries are from lateritic-type bauxites rather than karst-type
547 bauxites. Taking this into consideration, further work on characterising the REE
548 content in lateritic bauxites in Europe and in the known red mud storage facilities
549 across Europe would further refine any initial resource estimates.

550 5 Mt of red muds are currently 'dry' stacked at Aluminium S.A. in Greece while at
551 least 10 Mt of red muds are contained in the Seydişehir tailing ponds in Turkey, with
552 waste material being produced throughout the year. New data for REE in red muds
553 from stored waste facilities in Turkey and Greece demonstrate their potential as
554 REE resource. Total REE in red muds from the two sites is approximately 12000 t,
555 assuming an average of 1000 ppm REE in the red mud and an 80 % recovery (Borra
556 *et al.*, 2015).

557 **Discussion**

558 It is clear that red muds represent a significant potential resource of REE in Europe.
559 Understanding the REE content of red muds is essential for robust resource
560 estimation. Several factors may control the content and distribution of REE within
561 red muds. These include: 1) the REE content and mineralogy of the bauxite
562 precursor; and 2) the mineralogy of the REE within red mud ponds. The
563 development of industrial-scale processes to extract REE from red mud is
564 fundamental in establishing the economic viability of these potential resources.

565

566 *REE in bauxite and red mud*

567 The nature of, and mechanisms causing, variations in REE distribution in bauxites
568 are highly complicated with no one model fitting all deposits. In particular, the
569 effects of fractionation between the LREE and HREE, REE scavenging by Fe-rich
570 mineral phases, and changes in redox are not well understood. Although bauxites
571 are highly variable in their REE contents (e.g. from approximately 100 ppm to
572 greater than 2 300 ppm in bauxite from Parnassus-Giona (Laskou and Andreou,
573 2003)), in general there is often, but not always, an overall passive enrichment
574 downwards towards the limestone footwall. The importance of this is that REE
575 concentrations in red muds will be directly proportional to depth in the original
576 bauxite. If the original bauxite does not contain sufficient levels of REE, then REE
577 extraction from the red mud is unlikely to be viable, even with the recognised
578 enrichment factor of REE, including Sc and Y, from bauxite to red muds of
579 approximately 1:2 (Ochsenkühn-Petropoulou *et al.*, 1994; Wagh and Pinnock,
580 1987). Selection of red muds from processing of a particular bauxite horizon, or a
581 mixture of particular horizons, could potentially be carried out to produce ideal
582 blends for REE production.

583 The distribution and nature of the REE-bearing phases and minerals in red mud is

584 poorly defined. The association of REE with iron and manganese phases is widely
585 acknowledged in the literature, as is the presence of authigenic and detrital REE-
586 bearing minerals. However, much more work is necessary in order to fully
587 understand the distribution and mineralogy of REE in red muds. This will, in turn,
588 allow a clear economic quantification of the potential REE resources in European
589 red mud.

590

591 *REE processing*

592 Processing techniques for the two most common REE-containing minerals,
593 bastnäsite and monazite, are quite well understood and have well established
594 beneficiation flow sheets. Processing streams are being developed for other REE-
595 bearing minerals such as eudialyte (www.eurare.eu), however, these do not make
596 a significant contribution to current REE production (Jordens *et al.*, 2013). This
597 situation is likely to change with growing commercial demand for REE, with
598 increased opportunities to develop new rare earth element deposits with a wider
599 range and less well-understood mineralogy.

600 Successful extraction of REE from red muds has been achieved at both bench and
601 pilot scales (Wagh and Pinnock, 1987; Ochsenkühn-Petropoulou *et al.*, 1996, 2002;
602 Smirnov and Molchanova, 1997; Tsakanika *et al.*, 2004; Qu and Lian, 2013; RUSAL,
603 2014; Borra *et al.*, 2015). However, further development of these techniques is
604 necessary in order to make these resources economically viable. In order for REE to
605 be extracted most economically, ideally an additional processing stream for REE
606 would be developed as an add-on to the Bayer process itself.

607 Taking an average concentration of 1000 ppm REE for red muds, REE by-product
608 production from current, karst-bauxite sourced, alumina production,
609 approximately 1.5 Mt annually (BGS, 2015), could equate to up to 1500 t REE per

610 year. By-product production of REE from European bauxite exploitation of
611 appropriate deposits could result in a steady, secure supply of REE within Europe.
612 In order to benefit from the red muds that are currently stored onshore, it would
613 be advantageous to regard the re-mining of the tailing ponds as a viable additional
614 resource. It has been shown that it is not only the REE that are potential by-products
615 of the red muds, research is also on-going into the extraction of Ga and Sc
616 concentrates from red mud waste at Orbital Aluminae, Canada and Rusal, Russia,
617 respectively. Additionally, base metals and other critical raw materials are
618 frequently found in the waste material, depending on the original composition of
619 the source, and are potential by-products of further extractive processing.

620 One positive aspect of the onshore stockpiles of red muds in Europe is that these
621 are generally found in politically stable jurisdictions with an obvious history of
622 mining and therefore, possibly without strong local anti-mining sentiment.
623 Additionally, working on stockpiled waste is a more environmentally friendly option
624 as no additional mining, and minimal, if any, grinding, is required. It also could
625 provide an independent source of REE and protect REE-resource poor countries
626 from export quotas and price fluctuations (Binnemans and Jones, 2015).

627 The current lack of plant-scale methods of extracting REE from the red muds is a
628 potential obstacle to the development of these resources. Ongoing research, such
629 as that carried out by the FP7 funded EURARE and Mud2Metals projects, is tackling
630 these challenges. Under the recent patent granted to Orbite Aluminae Inc. (Patent
631 No. 14/371,364, Orbite, 2015) for the 'Orbite Process', a red mud processing plant
632 at Cap-Chat, Québec, Canada, is expected to begin production in the last quarter of
633 2015 and aims to produce a REE concentrate as one of the products. It also aims to
634 reprocess the red muds for alumina, as inefficiencies in the Bayer Process can result
635 in losses of up to 25% of the aluminium to the waste. The success of this

636 beneficiation stream could have a significant impact on the production of REE from
637 red mud waste. However, it has been shown that the extraction of REE from red
638 muds would do little to reduce the volume of red muds produced and so the
639 development of alternative uses for red muds is still a key societal and
640 environmental challenge (Klauber *et al.*, 2011).

641 There is a lack of collated data on red mud production and storage globally,
642 although it has been recognised internationally that the disposal, treatment and
643 maintenance of red mud ponds is of key social and environmental importance. This
644 issue was highlighted in 2010 with the tragic failure of the red mud pond at
645 Kolantár, Hungary. This has been addressed partly by the development of the
646 Bauxite, Residue and Disposal Database (BRaDD) (Gräfe *et al.*, 2011). Maintaining
647 and updating such a large database needs the support of industry but can aid in
648 developing an appropriate strategy for the management of red mud (Power *et al.*,
649 2011), including the possible extraction of valuable metallic commodities.

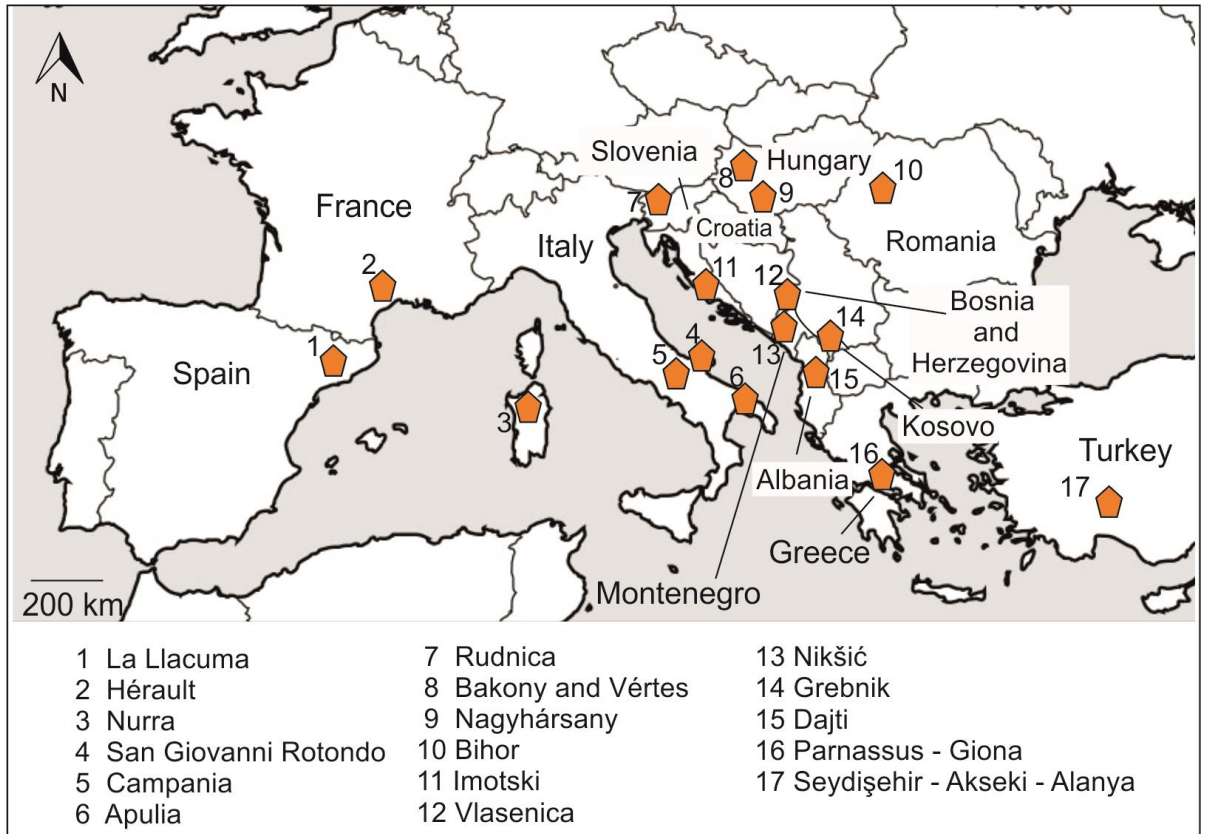
650 **Conclusions**

651 Potential resources of REE are present in significant quantities in red mud storage
652 facilities globally. Of these red muds, those that are derived from karst-type
653 bauxites are thought to be the most prospective for REE given the alkaline
654 conditions under which they form, where the pH due to the underlying limestone
655 retards mobility of the REE and traps the REE in the bauxite ore. In Europe, karst-
656 type bauxites are most common in the Mesozoic limestone of the Mediterranean.
657 Historic and current exploitation of these bauxite deposits has resulted in REE-
658 enriched red muds stored onshore across the region. This study has identified
659 combined potential resources of up to a maximum of 15000 tonnes REE contained
660 in red muds in two areas, one in Greece, the second in Turkey. A full exploration

661 campaign would be needed to investigate and evaluate the red mud waste tips. The
662 original heterogeneity of the bauxite could lead to heterogeneous waste tips that
663 would need careful resource estimation. Development of efficient beneficiation
664 and processing techniques and further work on understanding the distribution of
665 REE in red muds, in conjunction with the quantification of resources in European
666 red mud stocks, could lead to the development of sustainable REE production and
667 utilisation of waste material in Europe.

668 **Acknowledgments**

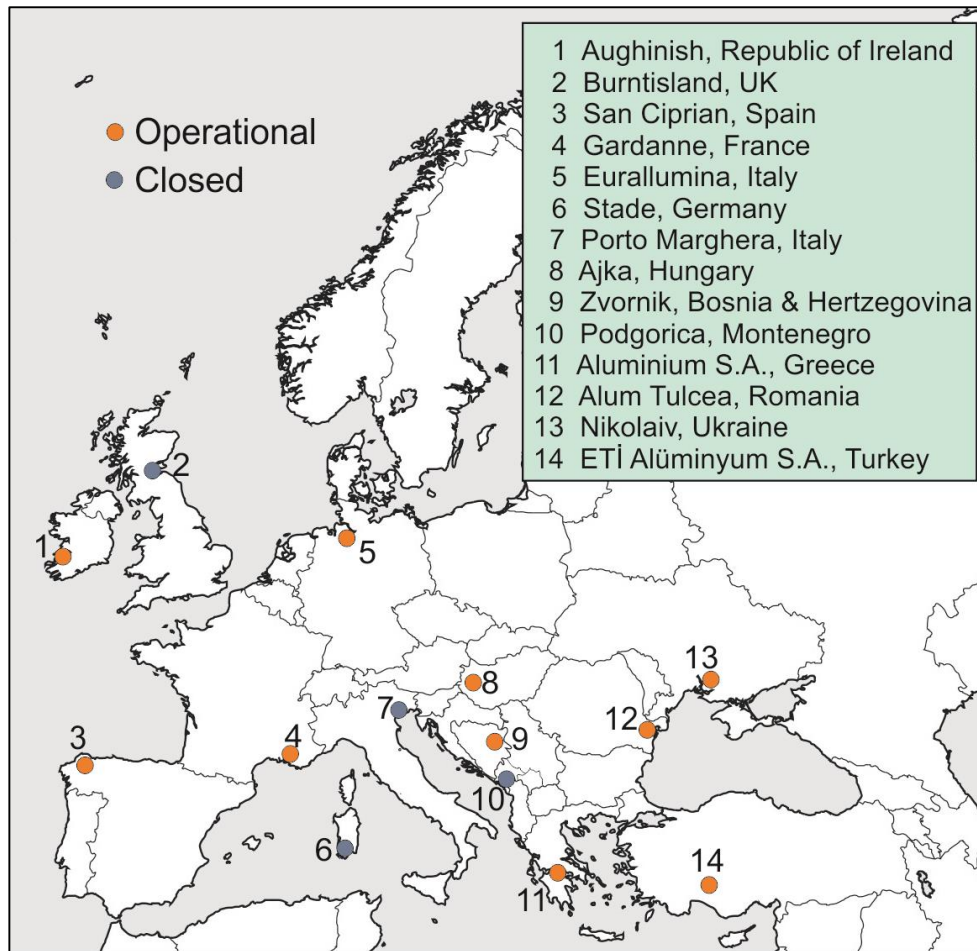
669 The research leading to these results has received funding from the European
670 Community's Seventh Framework Programme ([FP7/2007-2013]) under Grant
671 Agreement no. 309373. This publication reflects only the author's views, exempting
672 the Community from any liability. The authors would like to thank Aluminium S.A.
673 Greece and ETİ Alüminyum S.A., Turkey for providing bauxite and red mud samples.
674 The manuscript benefited greatly from the reviews of three anonymous reviewers.
675 É.D. and K.G. would like to thank Liam Hardy for aiding with sampling in Turkey. É.D.
676 and K.G. publish with the permission of the Executive Director, British Geological
677 Survey. British Geological Survey © NERC, all rights reserved [2015]. A.G. Gunn and
678 P.A. Lusty are thanked for their comments on the text. T. Barlow is thanked for
679 analysing red mud samples (Keyworth) and patiently explaining the corrections
680 applied to the ICP-MS data. D. Rayner is thanked for formatting figures. É.D. would
681 particularly like to thank Mr S. Griffin for asking 'how'.



682

683 Figure 1: European karst-bauxite deposits and mines in the circum-Mediterranean

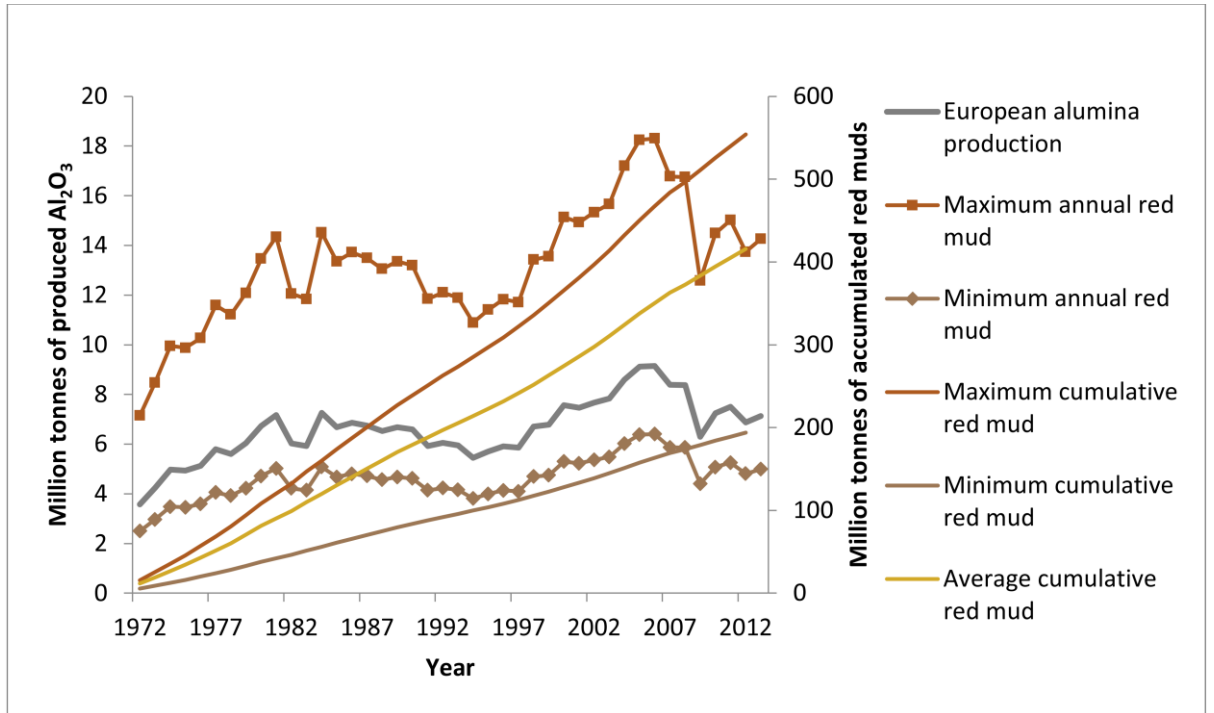
684 region (after Patterson, 1967).



685

686 Figure 2: Alumina refineries that utilise the Bayer process, both in use and
 687 abandoned in Europe (adapted after Power *et al.*, 2011).

688



689

690 Figure 3: Time series data of European alumina production since 1972 (data from

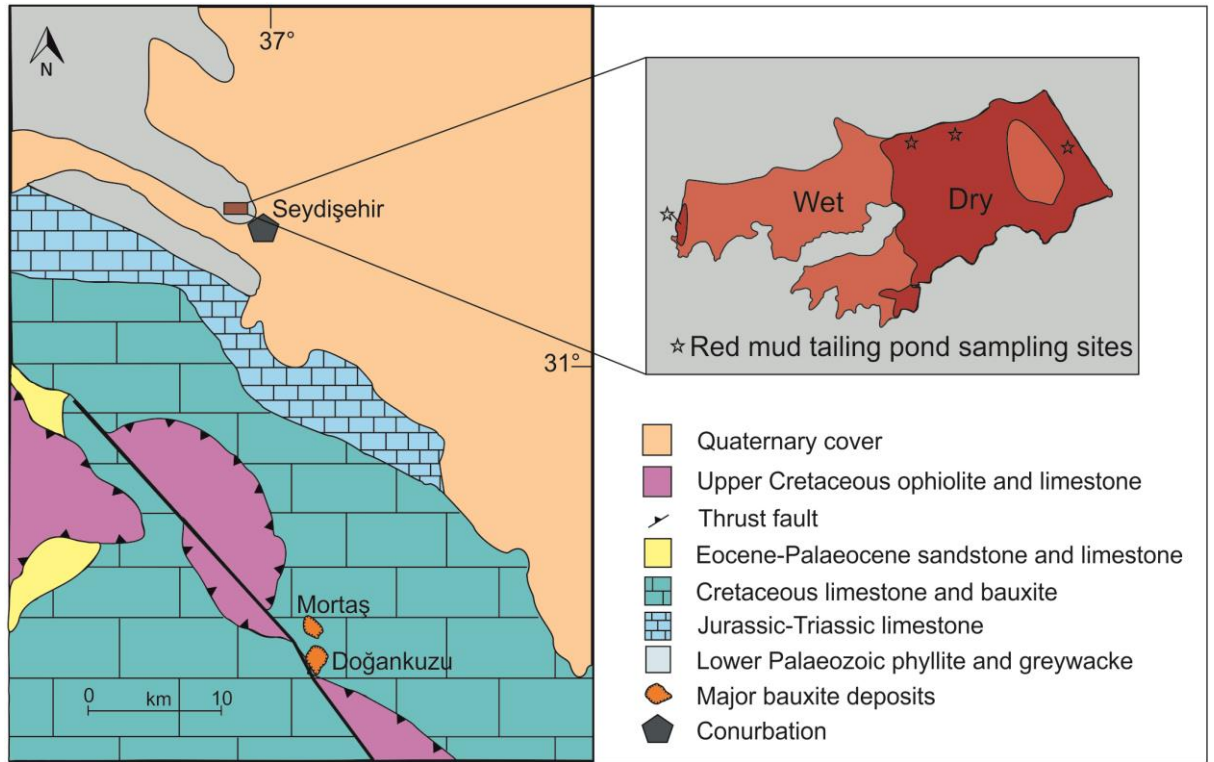
691 British Geological Survey World Mineral Statistics database). Greek data are

692 excluded before 2009 due to the disposal of red muds at sea. Annual European

693 alumina production is on the left-hand vertical axis, and cumulative average,

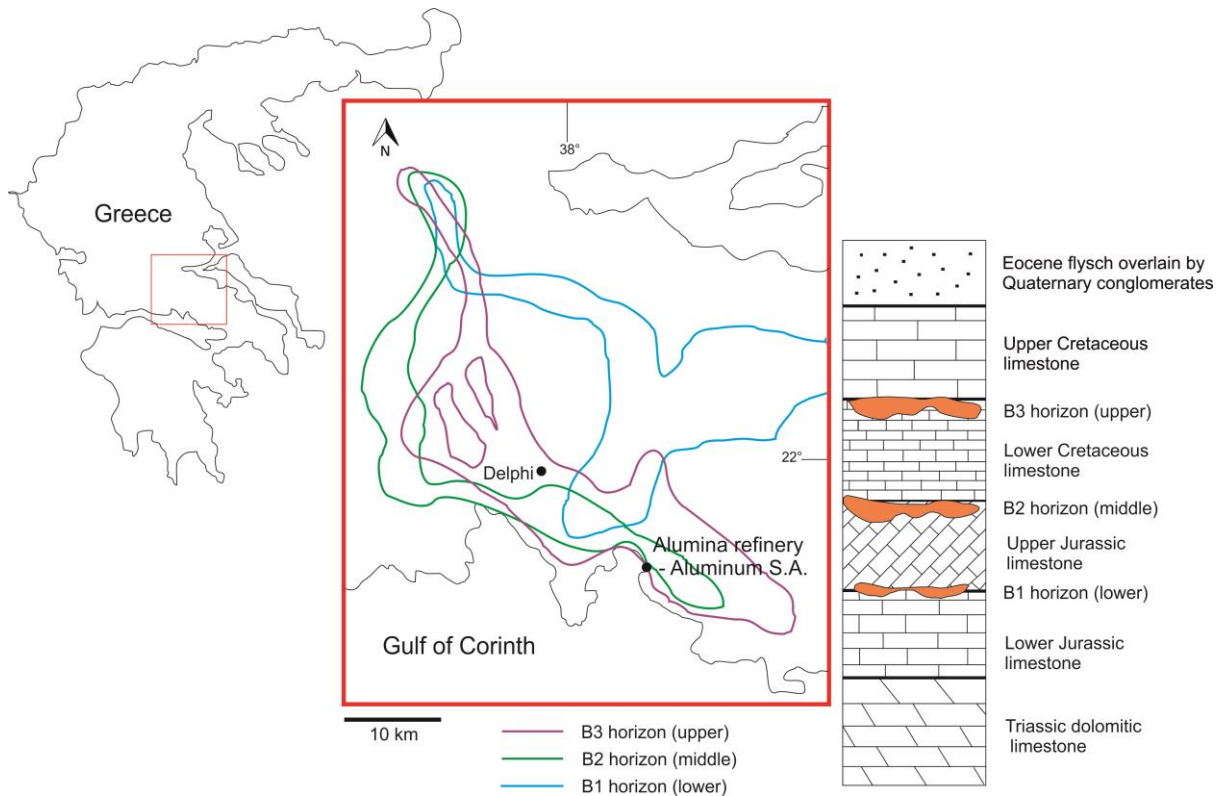
694 minimum and maximum volumes of red muds stored in European onshore tailing

695 ponds or 'dry' stacks are on the right-hand vertical axis.



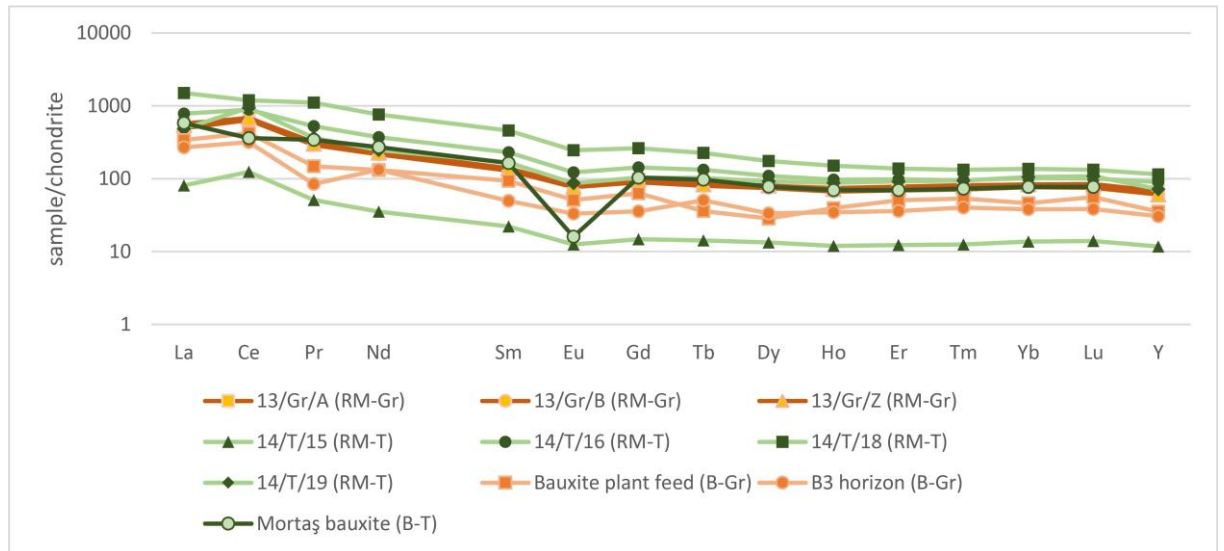
696

697 Figure 4: Geology of the Seydişehir area, Turkey (adapted with permission from
 698 Öztürk *et al.*, 2002 and *pers comm.*) showing key geological features, the location
 699 of the red mud tailing pond and sampling sites.



700

701 Figure 5: Regional distribution and simplified stratigraphic column of the three
 702 bauxite horizons (Petrascheck and Mack, 1978; Valeton *et al.*, 1987; schematic
 703 stratigraphic column reproduced with permission after Laskou and Economou-
 704 Eliopoulos, 2013).



705
 706 Figure 6: Chondrite-normalised (MacDonough and Sun, 1995) REE patterns for red
 707 mud samples from Greece and Turkey compared with published values for the
 708 Greek plant feed bauxite and the B3 horizon (Ochsenkühn-Petropoulou *et al.*,
 709 1994, 1995) and the Mortaş bauxite (Karadağ *et al.*, 2009). Red muds: RM;
 710 bauxites: B; Turkey: T; Greece: Gr.

Sample name	Red muds, this study							Bauxite, literature data					
	13/Gr/A	13/Gr/B	13/Gr/Z	14/T/15	14/T/16	14/T/18	14/T/19	Mortaş bauxite, Turkey*	Bolkardaği BP bauxite, Turkey*	Bolkardaği OS bauxite, Turkey*	Plant feed bauxite, (B3+B2) Greece*	Parnassus-Giona B3 bauxite, Greece*	Regia Piana bauxite, Italy (GBRX 8)*
	Parnassus-Giona red mud, Greece (this study)			Seydişehir red mud, Turkey (this study)									
La	134.9	117.2	129.3	19.2	185.9	356.2	114.8	137.6	107.6	35.8	80.2	64	87.7
Ce	416.9	391.3	421	76.1	543.2	728.5	576	221	233.5	159	259.5	195	154.1
Pr	29.6	27	28.3	4.7	49	102.7	33.9	31.7	24.7	7.1	13.8	7.8	19.7
Nd	107.4	99	104	16.2	169	346.7	113.5	124.7	88.1	26	59.8	60.3	74.2
Sm	20.5	19.1	20.5	3.3	34.1	67.9	24.7	24.2	17.2	5.2	13.8	7.3	13.4
Eu	4.5	4.3	4.4	0.7	6.9	13.8	4.9	0.9	3.8	1.2	2.8	1.8	2.8
Gd	19.3	17.8	19.6	0.5	4.8	8.2	3.7	20.6	17.9	6.4	12.5	7.1	12
Tb	3.1	2.8	3	2.9	28.5	52	20.6	3.5	3.2	1.4	1.3	1.8	2.1
Dy	19.7	18.2	19.9	3.3	27	42.9	22.7	19.1	19.6	9.6	7	8.2	11.9
Ho	4.1	3.6	3.9	0.7	5.3	8.2	4.8	3.8	4.2	2.3	2.1	1.9	2.5
Er	12.4	11	11.8	2	15.7	21.9	14.8	11.2	12.5	7.6	8	5.7	7.7
Tm	2	1.7	1.9	0.3	2.4	3.3	2.3	1.8	2	1.3	1.3	1	1.2
Yb	13.3	12.2	13.5	2.2	16.4	21.9	17	12.4	12.2	8.6	7.4	6.1	8.3
Lu	2.1	1.8	2.1	0.3	2.5	3.3	2.7	1.9	1.9	1.3	1.3	0.9	1.2
Total Lanthanoids	790	727.5	783.2	132.5	1090.6	1777.4	956.2	614.4	649.3	674.6	471.3	369.4	497.6
Y	106.2	95.4	95.2	18.4	141.3	180.2	112.7	N/A	78.2	126.2	55.4	48	56.7
TREE	896.2	822.8	878.4	150.9	1231.9	1957.5	1068.9	614.4	727.5	800.8	526.7	417.4	554.3

711

712 Table 1: REE (ppm) contents in red mud samples from Turkey and Greece,
713 (*literature data). Averaged values are for bauxite feed (a blend of horizons B3
714 and B2) from the Aluminium S.A. alumina refinery, Greece (Ochsenkühn-
715 Petropulu *et al.*, 1994, 1995); horizon three (B3) of the Parnassus-Giona bauxite
716 province, Greece (Valeton *et al.*, 1987; [Economopolou-Kyriakopoulou, 1991];
717 Laskou, 1991, 2005; Ochsenkühn-Petropoulou *et al.*, 1991; Laskou and Economou-
718 Eliopoulos, 2007, 2013); the Mortaş bauxite, Turkey (Karadağ *et al.*, 2009) and, for
719 comparison, the Baharpınarı (BP) and Öşün (OS) bauxite deposits in the Bolkardaği
720 bauxite province in Turkey (Hanilçı, 2013) and the Regia Piana bauxite (GBRX 8),
721 Italy (Boni *et al.*, 2013).

	Red mud (Mt)	TREE concentration (ppm) ^e	TREE content (Mt) (@ 50% recovery)	Nd concentration (ppm) ^e	Nd content (Mt) (@ 50% recovery)	HREE concentration (ppm) ^e	HREE content (Mt) (@ 50% recovery)
Minimum cumulative	200	1000	0.10	150	0.02	200	0.02

Maximum cumulative	550	1000	0.27	150	0.04	200	0.06
Average cumulative	425	1000	0.21	150	0.03	200	0.04

722

723 Table 2: Cumulative minimum, maximum and average tonnages of red muds
724 stored onshore in Europe since 1972 and their estimated contents of TREE; Nd;
725 and HREE_(Eu-Lu+Y); (^e estimate).

726 **References**

727 Akcil, A., Tuncuk, A., Okudan, D. and Deveci, H. (2013) Waste to resource:
728 evaluation of electrofiltration dust in Bayer Process. Pp. 75–80 in: *Proceedings of*
729 *the World Resources Forum 2013*, Davos, Switzerland, 6-9 October 2013.

730 Akinci, A. and Artir, R. (2008) Characterization of trace elements and radionuclides
731 and their risk assessment in red mud. *Materials Characterization*, **59**, 417–421.

732 Alonso, E., Sherman, A.M., Wallington, T.J., Everson, M.P., Field, F.R., Roth, R. and
733 Kirchain, R.E. (2012) Evaluating Rare Earth Element Availability: A Case with
734 Revolutionary Demand from Clean Technologies. *Environmental Science and*
735 *Technology*, **46**, 3406–3414.

736 Anagnostou, C. (2010) Bauxite resource exploitation in Greece vs. Sustainability.
737 Pp. 2425-2436 in: *Bulletin of the Geological Society of Greece*, **43**(5), *Proceedings*
738 *of the 12th International Congress, Patras, Greece*.

739 Anton, Á.D., Klebercz, O., Magyar, Á., Burke, I.T., Jarvis, A.P., Gruiz, K. and Mayes,
740 W.M. (2014) Geochemical recovery of the Torna–Marcal river system after the
741 Ajka red mud spill, Hungary. *Environmental Science: Processes & Impacts*, **16**,
742 2677–2685.

743 Atasoy, A. (2007) The comparison of the Bayer Process wastes on the base of
744 chemical and physical properties. *Journal of Thermal Analysis and Calorimetry*, **90**,
745 153–158.

746 Bárdossy, G. (1979) Growing significance of bauxites. *Episodes*, **2**, 22–25.

747 Bárdossy, G. (1982) *Karst Bauxites, Bauxite Deposits on Carbonate Rocks*. Elsevier,
748 444 pp.

749 Bárdossy, G. and Pantó, G. (1973) Trace mineral and element investigation on
750 bauxites by electron probe. Pp. 47–53 in: *3rd International Congress, ICSOBA*,
751 *(International Committee for Study of Bauxite, Alumina & Aluminium)*, Nice,
752 *France*.

753 Bárdossy, G., Panto, G. and Varhegyi, G. (1976) Rare metals in Hungarian bauxites
754 and conditions of their utilization. Pp. 221–231 in: *Travaux ICSOBA (International*
755 *Committee for Study of Bauxite, Alumina & Aluminium)*, Zagreb, Yugoslavia.

756 Binnemans, K. and Jones, P.T. (2015) Rare Earths and the Balance Problem.
757 *Journal of Sustainable Metallurgy*, **1**, 29–38.

758 Binnemans, K., Jones, P.T., Blanpain, B., Van Gerven, T., and Pontikes, Y. (2015)
759 Towards zero-waste valorisation of rare-earth-containing industrial process
760 residues: a critical review. *Journal of Cleaner Production*, **99**, 17-38.

761 Binnemans, K., Pontikes, Y., Jones, P.T., Van Gerven, T. and Blanpain, B. (2013a)
762 Recovery of rare earths from industrial waste residues: a concise review. Pp. 191–
763 205 in: *Proceedings of the Third International Slag Valorisation Symposium*.

764 Binnemans, K., Jones, P.T., Blanpain, B., Van Gerven, T., Yang, Y., Walton, A. and
765 Buchert, M. (2013b) Recycling of rare earths: a critical review. *Journal of Cleaner*
766 *Production*, **51**, 1–22.

767 Bland, W. and Rolls, D. (1998) *Weathering: An Introduction to the Scientific*
768 *Principles*. Arnold, 271 pp.

769 Bogatyrev, B.A., Zhukov, V. V. and Tsekhovskiy, Y.G. (2009) Formation conditions
770 and regularities of the distribution of large and superlarge bauxite deposits.
771 *Lithology and Mineral Resources*, **44**, 135–151.

772 Boni, M., Rollinson, G., Mondillo, N., Balassone, G. and Santoro, L. (2013)
773 Quantitative mineralogical characterization of karst bauxite deposits in the
774 southern Apennines, Italy. *Economic Geology*, **108**, 813–833.

775 Borra, C.R., Pontikes, Y., Binnemans, K. and Van Gerven, T. (2015) Leaching of rare
776 earths from bauxite residue (red mud). *Minerals Engineering*, **76**, 20–27.

777 Bosák, P., Ford, D., Głazek, J. and Horáček, I. (1989) *Paleokarst a systematic and*
778 *regional review*. Elsevier, 725 pp.

779 Bourbos, E., Giannopoulou, I., Karatonis, A., Pantias, D. and Paspaliaris, I. (2014)
780 Electrodisposition of rare earth metals in ionic liquids. Pp. 156–162 in: *ERES2014:*
781 *1st European Rare Earth Resources Conference, Milos, 04-07/09/2014*.

782 British Geological Survey. (2012) *Risk List 2012*.

783 British Geological Survey. (2015) *World mineral production 2009-2013*. Keyworth,
784 Nottingham: British Geological Survey.

785 CREEN (Canadian Rare Earth Elements Research Network). (2013) *Progress Report*
786 *Number 1*.

787 Davris, P., Balomenos, E. and Panias, D. (2014) Leaching of rare earths from
788 bauxite residues using imidazolium based ionic liquids. Pp. 241–252 in: *ERES2014:*
789 *1st European Rare Earth Resources Conference, Milos, 04-07/09/2014.*

790 Derevyankin, V.A., Porotnikova, T.P., Kocherova, E.K., Yumasheva, I.V. and
791 Moiseev, V.E. (1981) Behaviour of scandium and lanthanum in the production of
792 alumina from bauxite. *Izvestiya Vysshikh Uchebnykh Zavedenii, Tsvetnaya*
793 *Metallurgiya*, 86–89.

794 Doutsos, T., Koukouvelas, I.K. and Xypolias, P. (2006) A new orogenic model for
795 the External Hellenides. Pp. 507–520 in: *Tectonic Development of the Eastern*
796 *Mediterranean Region Geological Society, London, Special Publications 260(1).*

797 Economopoulou-Kyriakopoulou, N. (1991) A comparative geochemical and
798 mineralogical study of bauxitic horizons in central Greece, PhD Thesis, National
799 Technical University of Athens, Faculty of Mining Engineering and Metallurgy. 119
800 pp.

801 European Commission. (2013) *Critical Metals in the Path towards the*
802 *Decarbonisation of the EU Energy Sector*. 244 pp.

803 European Commission. (2014) *Report on critical raw materials for the EU Report of*
804 *the ad hoc working group on defining critical raw materials*. 41 pp.

805 Fleet, A.J. (1984) Aqueous and sedimentary geochemistry of the rare earth
806 elements. Pp. 343–373 in: *Rare Earth Element Geochemistry* (P. Henderson,
807 editor). Elsevier.

808 Gamaletsos, P., Godelitsas, A., Chatzitheodoridis, E. and Kostopoulou, D. (2007)
809 Laser μ -ramen investigation of Greek bauxites from the Parnassos-Ghiona active

810 mining area. Pp. 736-746 in: *Bulletin of the Geological Society of Greece*, **40**(2),
811 *Proceedings of the 11th International Congress, Athens, Greece.*

812 Gelencsér, A., Kováts, N., Turóczy, B., Rostási, Á., Hoffer, A., Imre, K., Nyiró-Kósa, I.,
813 Csákberényi-Malasics, D., Tóth, Á., Czitrovsky, A., Nagy, A., Nagy, S., Ács, A.,
814 Kovács, A., Ferincz, Á., Hartyáni, Z. and Pósfai, M. (2011) The red mud accident in
815 Ajka (Hungary): Characterization and potential health effects of fugitive dust.
816 *Environmental Science and Technology*, **45**, 1608–1615.

817 Goodenough, K.M., Schilling, J., Jonsson, E., Kalvig, P., Charles, N., Tuduri, J.,
818 Deady, É.A., Sadeghi, M., Schiellerup, H., Müller, A., Bertrand, G., Arvanitidis, N.,
819 Eliopoulos, D.G., Shaw, R.A., Thrane, K. and Keulen, N. (2016) Europe’s rare earth
820 resource potential: an overview of metallogenic provinces and their geodynamic
821 setting. *Ore Geology Reviews*, **72**, 838-856.

822 Gow, N. N., Lozej, G.P. (1993) Bauxite. *Geoscience Canada*, **20**, 9–16.

823 Graedel, T.E. (2014) Metal resources, use and criticality. Pp. 1–19 in: *Critical*
824 *Metals Handbook* (G. Gunn, editor). First Edit. John Wiley & Sons, Ltd.

825 Gräfe, M. and Klauber, C. (2011) Bauxite residue issues: IV. Old obstacles and new
826 pathways for in situ residue bioremediation. *Hydrometallurgy*, **108**, 46–59.

827 Hamada, T. (1986) Environmental management of bauxite residue. Pp. 109–117
828 in: *Proceedings of the International Conference on Bauxite Tailings. The Jamaica*
829 *Bauxite Institute, The University of the West Indies, Kingston, Jamaica.*

830 Haniççi, N. (2013) Geological and geochemical evolution of the Bolkardaği bauxite
831 deposits, Karaman, Turkey: Transformation from shale to bauxite. *Journal of*
832 *Geochemical Exploration*, **133**, 118–137.

833 Hatch, G.P. (2012) Dynamics in the global market for rare earths. *Elements*, **8**,
834 341–346.

835 Hind, A.R., Bhargava, S.K. and Grocott, S.C. (1999) The surface chemistry of Bayer
836 process solids: a review. *Colloids and Surfaces A: Physicochemical and Engineering*
837 *Aspects*, **146**, 359–374.

838 Horkel, A. (2010) Notes on the geology and minerals resource potential of
839 selected Turkish bauxite deposits. *Jahrbuch der Geologischen Bundesanstalt*, **150**,
840 343–350.

841 Humphries, M. (2013) *Rare Earth Elements: The Global Supply Chain*.
842 Congressional Research Service report no. 41347. 31 pp.

843 Institute of Geological Sciences. (1978) *World Mineral Statistics 1970-74*.

844 International Aluminium Institute. (2014) *Bauxite Residue Management: Best*
845 *Practice*. 32 pp.

846 International Marine Organisation. (1972) International Convention on the
847 Prevention of Marine Pollution by Dumping of Wastes and Other Matter.

848 Johannesson, K.H., Lyons, W.B., Stetzenbach, K.J. and Byrne, R.H. (1995) The
849 solubility control of rare earth elements in natural terrestrial waters and the
850 significance of PO₄³⁻ and CO₃²⁻ in limiting dissolved rare earth concentrations: a
851 review of recent information. *Aquatic Geochemistry*, **1**, 157–173.

852 Johannesson, K.H., Stetzenbach, K.J., Hodge, V.F. and Lyons, W.B. (1996) Rare
853 earth element complexation behavior in circumneutral pH groundwaters:
854 assessing the role of carbonate and phosphate ions. *Earth Planet Science Letters*,
855 **139**, 305–319.

856 Jordens, A., Cheng, Y.P. and Waters, K.E. (2013) A review of the beneficiation of
857 rare earth element bearing minerals. *Minerals Engineering*, **41**, 97–114.

858 Kalaitzidis, S., Siavalas, G., Skarpelis, N., Araujo, C.V. and Christanis, K. (2010) Late
859 Cretaceous coal overlying karstic bauxite deposits in the Parnassus-Ghiona Unit,
860 Central Greece: Coal characteristics and depositional environment. *International
861 Journal of Coal Geology*, **81**, 211–226.

862 Karadağ, M.M., Küpeli, Ş., Arýk, F., Ayhan, A., Zedef, V. and Döyen, A. (2009) Rare
863 earth element (REE) geochemistry and genetic implications of the Mortaş bauxite
864 deposit (Seydişehir/Konya - Southern Turkey). *Chemie der Erde - Geochemistry*,
865 **69**, 143–159.

866 Klauber, C., Gräfe, M. and Power, G. (2011) Bauxite residue issues: II. options for
867 residue utilization. *Hydrometallurgy*, **108**, 11–32.

868 Klyucharev, D.S., Volkova, N.M. and Comyn, M.F. (2013) The problems associated
869 with using non-conventional rare-earth minerals. *Journal of Geochemical
870 Exploration*, **133**, 138–148.

871 Laskou, M. (1991) Concentrations of rare earths in Greek Bauxites. *Acta Geologica
872 Hungarica*, **34**, 395–404.

873 Laskou, M. (2005) Pyrite-rich bauxites from the Parnassos-Ghiona zone, Greece.
874 Pp. 1007–1010 in: *8th SGA Meeting, Mineral Deposits Research Meeting the
875 Global Challenge, Beijing, August 18-21*.

876 Laskou, M. and Economou-Eliopoulos, M. (2007) The role of microorganisms on
877 the mineralogical and geochemical characteristics of the Parnassos-Ghiona
878 bauxite deposits, Greece. *Journal of Geochemical Exploration*, **93**, 67–77.

879 Laskou, M. and Economou-Eliopoulos, M. (2013) Bio-mineralization and potential
880 biogeochemical processes in bauxite deposits: Genetic and ore quality
881 significance. *Mineralogy and Petrology*, **107**, 471–486.

882 Laskou, M., Economou-Eliopoulos, M. and Mitsis, I. (2010) Bauxite ore as an
883 energy source for bacteria driving iron-leaching and bio-mineralization. *Hellenic*
884 *Journal of Geosciences*, **45**, 163–174.

885 Laskou, M., and Andreou, G. (2003) Rare earth elements distribution and REE-
886 minerals from the Parnassos- Ghiona bauxite deposits, Greece. Pp. 89–92 in:
887 *Mineral Exploration and Sustainable Development: Proceedings of the Seventh*
888 *Biennial SGA Meeting, Athens, Greece, 24-28 August 2003, Volume 2*.

889 Lympelopoulou, T. (1996) Determination and extraction of rare earth elements
890 from bauxites and red mud. 183 pp. (unpublished doctoral thesis, National
891 Technical University of Athens (NTUA), 1996).

892 Maksimović, Z. and Pantó, G. (1978) Minerals of the rare-earth elements in karstic
893 bauxites: synchysite-(Nd), a new mineral from Grebnik deposit. Pp. 540–552 in:
894 *4th International Congress, ICSOBA, (International Committee for Study of Bauxite,*
895 *Alumina & Aluminium), Athens, Greece*.

896 Maksimović, Z. and Panto, G. (1991) Contribution to the geochemistry of the rare
897 earth elements in the karst-bauxite deposits of Yugoslavia and Greece. *Geoderma*,
898 **51**, 93–109.

899 Maksimović, Z. and Pantó, G. (1996) Authigenic rare earth minerals in karst-
900 bauxites and karstic nickel deposits. Pp. 257–259 in: *Rare Earth Minerals,*
901 *Chemistry, Origin and Ore Deposits*. Volume 7. (F.A. Jones, F. Wall and C.T.
902 Williams, editors). First Edit. Springer Science & Business Media.

903 Maksimović, Z. and Roaldset, E. (1976) Lanthanide elements in some
904 Mediterranean karstic bauxite deposits. Pp. 199–220 in: *Travaux ICSOBA*,
905 (*International Committee for Study of Bauxite, Alumina & Aluminium*), Zagreb,
906 *Croatia*.

907 Mameli, P., Mongelli, G., Oggiano, G. and Dinelli, E. (2007) Geological,
908 geochemical and mineralogical features of some bauxite deposits from Nurra
909 (Western Sardinia, Italy): Insights on conditions of formation and parental affinity.
910 *International Journal of Earth Sciences*, **96**, 887–902.

911 Marmolejo-Rodríguez, A.J., Prego, R., Meyer-Willerer, A., Shumilin, E. and
912 Sapozhnikov, D. (2007) Rare earth elements in iron oxy–hydroxide rich sediments
913 from the Marabasco River-Estuary System (pacific coast of Mexico). REE affinity
914 with iron and aluminium. *Journal of Geochemical Exploration*, **94**, 43–51.

915 McDonough W. F., and Sun, S. -s. (1995) The composition of the Earth. *Chemical*
916 *Geology*, **120**, 223–253.

917 Melfos, V. and Voudouris, P.C. (2012) Geological, Mineralogical and Geochemical
918 Aspects for Critical and Rare Metals in Greece. *Minerals*, **2**, 300–317.

919 Milačić, R., Zuliani, T. and Ščančar, J. (2012) Environmental impact of toxic
920 elements in red mud studied by fractionation and speciation procedures. *Science*
921 *of the Total Environment*, **426**, 359–365.

922 Mitsubishi Electric Corporation. (2014) There are not enough rare earth elements
923 for cutting-edge industries.
924 ([http://www.mitsubishielectric.com/company/environment/ecotopics/rareearth/](http://www.mitsubishielectric.com/company/environment/ecotopics/rareearth/why/index.html)
925 [why/index.html](http://www.mitsubishielectric.com/company/environment/ecotopics/rareearth/why/index.html) accessed February 2015).

926 Mondillo, N., Balassone, G., Boni, M. and Rollinson, G. (2011) Karst bauxites in the
927 Campania Apennines (southern Italy): A new approach. *Periodico di Mineralogia*,
928 **80**, 407–432.

929 Mongelli, G. (1997) Ce-anomalies in the textural components of Upper Cretaceous
930 karst bauxites from the Apulian carbonate platform (southern Italy). *Chemical*
931 *Geology*, **140**, 69–79.

932 Mongelli, G. and Acquafredda, P. (1999) Ferruginous concretions in a Late
933 Cretaceous karst bauxite: composition and conditions of formation. *Chemical*
934 *Geology*, **158**, 315–320.

935 Mongelli, G., Boni, M., Buccione, R. and Sinisi, R. (2014) Geochemistry of the
936 Apulian karst bauxites (southern Italy): Chemical fractionation and parental
937 affinities. *Ore Geology Reviews*, **63**, 9–21. Elsevier B.V.

938 Nesbitt, H.W. (1979) Mobility and fractionation of rare earth elements during
939 weathering of a granodiorite. *Nature*, **279**, 206–210.

940 O’ Driscoll, M. (2011) Elmin bauxite sees the light. *Industrial Minerals*, **3**, 42–45.

941 Ochsenkühn-Petropoulou, M., Ochsenkühn, K. and Luck, J. (1991) Comparison of
942 inductively coupled plasma mass spectrometry with inductively coupled plasma
943 atomic emission spectrometry and instrumental neutron activation analysis for
944 the determination of rare earth elements in Greek bauxites. *Spectrochimica Acta*
945 *Part B: Atomic Spectroscopy*, **46**, 51–65.

946 Ochsenkühn-Petropulu, M., Lyberopulu, T. and Parissakis, G. (1994) Direct
947 determination of lanthanides, yttrium and scandium in bauxites and red mud
948 from alumina production. *Analytica Chimica Acta*, **296**, 305–313.

949 Ochsenkühn-Petropulu, M., Lyberopulu, T. and Parissakis, G. (1995) Selective
950 separation and determination of scandium from yttrium and lanthanides in red
951 mud by a combined ion exchange/solvent extraction method. *Analytica Chimica*
952 *Acta*, **315**, 231–237.

953 Ochsenkühn-Petropulu, M., Lyberopulu, T., Ochsenkühn, K.M. and Parissakis, G.
954 (1996) Recovery of lanthanides and yttrium from red mud by selective leaching.
955 *Analytica Chimica Acta*, **319**, 249–254.

956 Ochsenkühn-Petropulu, M., Hatzilyberis, K.S., Mendrinous L.N. and Salmas, C.E.
957 (2002) Pilot-plant investigation of the leaching process for the recovery of
958 scandium from red mud. *Industrial and Engineering Chemistry Research*, **41**, 5749-
959 5801

960 Ohta, A. and Kawabe, I. (2001) REE(III) adsorption onto Mn dioxide (δ -MnO₂) and
961 Fe oxyhydroxide: Ce(III) oxidation by δ -MnO₂. *Geochimica et Cosmochimica Acta*,
962 **65**, 695–703.

963 Okay, A.I. (2008) Geology of Turkey: A synopsis. *Anschnitt*, **21**, 19–42.

964 Orbite Aluminae Incorporated. (2015) Process for Extracting Aluminum from
965 Aluminous Ores. Patent No. 14/371,364.

966 Öztürk, H., Hein, J., Haniççi, N. (2002) Genesis of the Doğankuzu and Mortaş
967 bauxite deposits, Taurides, Turkey: Separation of Al, Fe, and Mn and implications
968 for passive margin metallogeny. *Economic Geology*, **97**, 1063–1077.

969 Patterson, S.H. (1967) *Bauxite reserves and potential aluminum resources of the*
970 *World*. 184 pp. Bulletin No. 1228. US Government Print Office.

971 Petrascheck, W.E. (1989) The genesis of allochthonous karst-type bauxite deposits
972 of southern Europe. *Mineralium Deposita*, **81**, 77–81.

973 Petrascheck, W.E. and Mack, E. (1978) Palaeogeographie, verteilung und qualität
974 der bauxite im Parnass-Kjona Gebirge. Pp. 526–539 in: *4th International Congress,*
975 *ICSOBA, (International Committee for Study of Bauxite, Alumina & Aluminium),*
976 *Athens, Greece.*

977 Power, G., Gräfe, M. and Klauber, C. (2011) Bauxite residue issues: I. Current
978 management, disposal and storage practices. *Hydrometallurgy*, **108**, 33–45.

979 Qu, Y. and Lian, B. (2013) Bioleaching of rare earth and radioactive elements from
980 red mud using *Penicillium tricolor* RM-10. *Bioresource Technology*, **136**, 16–23.

981 Ritter, S. (2014) Making the most of red mud. *Chemical and Engineering News*, **92**,
982 33–35.

983 Robertson, A.H.F. and Mountrakis, D. (2006) Tectonic development of the Eastern
984 Mediterranean region: an introduction. Pp. 1–9 in: *Tectonic Development of the*
985 *Eastern Mediterranean Region Geological Society, London, Special Publications*
986 260(1).

987 RUSAL. (2014) UC RUSAL launches pilot unit at Urals aluminium smelter for the
988 production of scandium concentrate. [press release]
989 (http://www.rusal.ru/en/press-center/news_details.aspx?id=10866&ibt=13
990 accessed February 2015)

991 Sengör, A.M.C. and Yilmaz, Y. (1981) Tethyan evolution of Turkey: A plate tectonic
992 approach. *Tectonophysics*, **75**, 181–241.

993 Simandl, G.J. (2014) Geology and market-dependent significance of rare earth
994 element resources. *Mineralium Deposita*, 889–904.

995 Smirnov, D.I. and Molchanova, T.V. (1997) The investigation of sulphuric acid
996 sorption recovery of scandium and uranium from the red mud of alumina
997 production. *Hydrometallurgy*, **45**, 249–259.

998 Temur, S., Orhan, H. and Deli, A. (2009) Geochemistry of the limestone of Mortaş
999 Formation and related terra rossa, Seydişehir, Konya, Turkey. *Geochemistry
1000 International*, **47**, 67–93.

1001 Tsakanika, L. V., Ochsenkühn-Petropoulou, M.T. and Mendrinou, L.N. (2004)
1002 Investigation of the separation of scandium and rare earth elements from red
1003 mud by use of reversed-phase HPLC. *Analytical and Bioanalytical Chemistry*, **379**,
1004 796–802.

1005 Tsirambides, A. and Filippidis, A. (2012) Metallic mineral resources of Greece.
1006 *Central European Journal of Geosciences*, **4**, 641–650.

1007 Valetou, I., Biermann, M., Reche, R. and Rosenberg, F. (1987) Genesis of nickel
1008 laterites and bauxites in Greece during the Jurassic and Cretaceous, and their
1009 relation to ultrabasic parent rocks. *Ore Geology Reviews*, **2**, 359–404.

1010 Vukotić, P. (1983) Determination of rare earth elements in bauxites by
1011 instrumental neutron activation analysis. *Journal of Radioanalytical Chemistry*, **78**,
1012 105–115.

1013 Wagh, A.S. and Pinnock, W.R. (1987) Occurrence of scandium and rare earth
1014 elements in Jamaican bauxite waste. *Economic Geology*, **82**, 757–761.

- 1015 Wall, F. (2014) Rare earth elements. Pp. 312–339 in: *Critical Metals Handbook* (G. Gunn, editor). First Edit. John Wiley & Sons, Ltd.
- 1016